GPS WORLD
GNSS POSITION NAVIGATION TIMING
WWW.GPSWORLD.COM

Innovation

Relative Positioning with RTK Filtering and PPP

FILLING THE GAPS

SPECIAL SIMULATOR ISSUE

SIGNALS OF OPPORTUNITY OFFSET SATELLITE LIMITATIONS

SURVEY & MAPPING: PHONE SYNERGY

UAV: GAS-LEAK DETECTION

PNT ROUNDUP: INERTIAL, WI-FI

POSITION UNCERTAINTY WITH FIVE SATELLITES (YELLOW). ADD THREE CELLULAR SIGNALS (BLUE).

OPPORTUNITY FOR ACCURACY

EXPLOITING TERRESTRIAL SIGNALS OF OPPORTUNITY

(SOPs) can significantly reduce the vertical dilution of precision (VDOP) of a GNSS navigation solution. Simulation and experimental results show that that adding cellular SOP observables is more effective in reducing VDOP than adding GNSS space vehicle (SV) observables.

BY **Joshua J. Morales, Joe J. Khalife and Zaher M. Kassas**

GNSS position solutions can in many cases suffer from a high vertical dilution of precision (VDOP) due to lack of space vehicle (SV) angle diversity. Signals of opportunity (SOPs) have been recently considered to enable navigation whenever GNSS signals become inaccessible or untrustworthy. Terrestrial SOPs are abundant and are available at varying geometric configurations, making them an attractive supplement to GNSS for reducing VDOP.

Common metrics used to assess the quality of the spatial geometry of GNSS SVs are the parameters of the geometric dilution of precision (GDOP); namely, horizontal dilution of precision (HDOP), time dilution of precision (TDOP), and VDOP. Several methods have been investigated for selecting the best GNSS SV configuration to improve the navigation solution by minimizing the GDOP. While the navigation solution is always improved by additional observables from GNSS SVs, the solution's VDOP generally remains of lesser quality than the HDOP. GPS augmentation with terrestrial transmitters that transmit GPS-like signals have been shown to reduce VDOP. However, this requires installation of additional proprietary infrastructure.

This article studies VDOP reduction by exploiting terrestrial SOPs, particularly cellular code division multiple access (CDMA) signals, which have inherently low elevation angles and are free to use.

In GNSS-based navigation, the states of the SVs are readily available. For SOPs, however, even though the position states may be known a priori, the clock-error states are dynamic; hence, they must be continuously estimated. The states of SOPs can be made available through one or more receivers in the navigating receiver's vicinity. Here, the estimates of such SOPs are exploited and the VDOP reduction is evaluated.

PROBLEM FORMULATION

Consider an environment comprising a receiver, M GNSS SVs, and N terrestrial SOPs. Each SOP will be assumed to emanate from a spatially stationary transmitter, and its state vector, $x_{sop(n)}$, will consist of its three-dimensional (3-D) position $r_{sop(n)}$ and clock bias $c\delta t_{sop(n)}$, where $n=1,\ldots,N$ and c is the speed of light. The receiver draws pseudorange observations from the GNSS SVs and from the SOPs. The observations are fused through an estimator whose role is to estimate the state vector of the receiver $x_r=[r_r^T,\ c\delta t_r]^T$, where r_r and $c\delta t_r$ are the 3D position and clock bias of the receiver, respectively. To simplify the discussion, assume that the pseudorange observation noise is independent and identically distributed across all channels with variance σ^2. The estimator produces an estimate of the receiver's state vector $\hat{x}_r$ and associated estimation error covariance $P=\sigma^2(H^TH)^{-1}$.

Without loss of generality, assume an East-North-Up (ENU) coordinate frame to be centered at $\hat{x}_r$. In this frame, the dilution of precision matrix $G\equiv(H^TH)^{-1}$ is completely determined by the azimuth and elevation angles from the receiver to each SV, denoted $az_{sv(m)}$ and $el_{sv(m)}$, respectively, and the receiver to each SOP, denoted $az_{sop(n)}$ and $el_{sop(n)}$, respectively, where $m=1,\ldots,M$. Hence, the quality of the estimate depends on these angles and the pseudorange observation noise variance σ^2. The diagonal elements of G, denoted g_{ii}, are the parameters of the dilution of precision (DOP) factors:

$$\text{GDOP} \equiv \sqrt{tr[G]}$$

$$\text{HDOP} \equiv \sqrt{g_{11}+g_{22}}$$

$$\text{VDOP} \equiv \sqrt{g_{33}}$$

Therefore, the DOP values are directly related to the estimation error covariance; hence, the more favorable the azimuth and elevation angles, the lower the DOP values. If the observation noise was not independent and identically distributed, the weighted DOP factors must be used.

VDOP REDUCTION VIA SOPs

With the exception of GNSS receivers mounted on high-flying and space vehicles, all GNSS SVs are typically above the receiver, that is, the receiver-to-SV elevation

	M=4		M=5		M=6		M=7	
(m)	az_{sv_m}	el_{sv_m}	az_{sv_m}	el_{sv_m}	az_{sv_m}	el_{sv_m}	az_{sv_m}	el_{sv_m}
1	185	79	189	66	46	40	61	21
2	52	60	73	69	101	58	57	49
3	326	52	320	41	173	59	174	30
4	242	47	56	27	185	38	179	66
5	-	-	261	51	278	67	269	31
6	-	-	-	-	314	41	218	56
7	-	-	-	-	-	-	339	62

TABLE 1 SV azimuth and elevation angle (degrees).

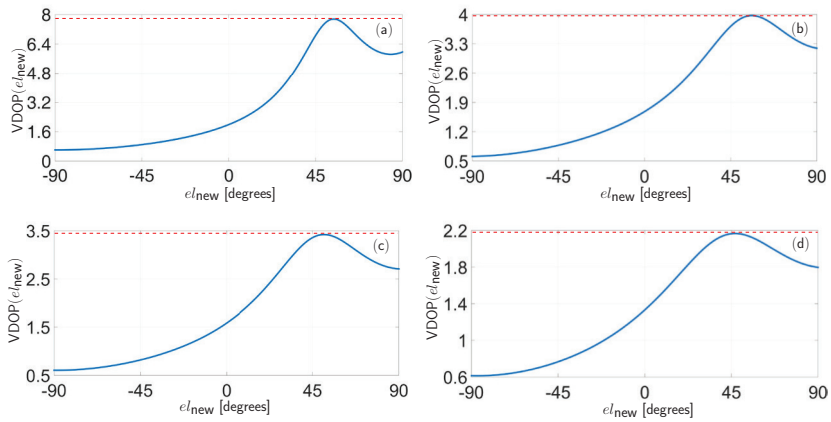

FIGURE 1 A receiver has access to M GPS SVs from Table I. Plots (a)- (d) show the VDOP for each GPS SV configuration before adding an additional measurement (red dotted line) and the resulting VDOP(el_{new}) for adding an additional measurement (blue curve) at an elevation angle $-90° \le el_{new} \le 90°$ for $M=4,\ldots,7$, respectively.

angles are theoretically limited between $0° \le el_{sv(m)} \le 90°$. GNSS receivers typically restrict the lowest elevation angle to some elevation mask, $el_{sv,min}$, so to ignore GNSS SV signals that are heavily degraded due to the ionosphere, troposphere and multipath. As a consequence, GNSS SV observables lack elevation angle diversity, and the VDOP of a GNSS-based navigation solution is degraded. For ground vehicles, $el_{sv,min}$ is typically between 5° and 20°. These elevation angle masks also apply to low-flying aircraft, such as small unmanned aerial vehicles (UAVs), whose flight altitudes are limited to 500 feet (approximately 152 meters) by the Federal Aviation Administration (FAA).

In GNSS + SOP-based navigation, the elevation angle span may effectively double, specifically $-90° \le el_{sop(n)} \le 90°$. For ground vehicles, useful observations can be made on terrestrial SOPs that reside at elevation angles of $el_{sop(n)}=0°$. For aerial vehicles, terrestrial SOPs can reside at elevation angles as low as $el_{sop(n)}=-90°$, for example, if the vehicle is flying directly above the SOP transmitter.

To illustrate the VDOP reduction by incorporating additional GNSS SV observations versus additional SOP observations, an additional observation at el_{new} is introduced, and the resulting VDOP(el_{new}) is evaluated. To this end, M SV azimuth and elevation angles were computed using GPS ephemeris files accessed from the Yucaipa, California, station from Garner GPS Archive, which are tabulated in **TABLE 1**. For each set of GPS SVs, the azimuth angle of an additional observation was chosen as a random sample from a uniform distribution between 0° and 360°, that is, $az_{new} \sim U(0°,360°)$. The corresponding VDOP for introducing an additional measurement at a sweeping elevation angle $-90° \le el_{new} \le 90°$ are plotted in **FIGURE 1 (a)–(d)** for $M=4,\ldots,7$, respectively.

The following can be concluded from these plots. First, while the VDOP is always improved by introducing an additional measurement, the improvement of adding an SOP measurement is much more significant than adding an additional GPS SV measurement. Second, for elevation angles inherent only to terrestrial SOPs, that is, $-90° \le el_{sop(n)} \le 0°$, the VDOP is monotonically decreasing for decreasing elevation angles.

SIMULATION RESULTS

To compare the VDOP of a GNSS-only navigation solution with a GNSS + SOP navigation solution,

www.ifen.com

Spoofing Testing

NavX®-NCS Professional GPS/GNSS Simulator

GPS | GLONASS | Galileo | BeiDou | IRNSS | QZSS | SBAS

- Unique flexibility with up to 9 RF frequencies simultaneously
- Outstanding scalability with up to 108 signal channels
- 4 RF signal outputs for beam-forming applications
- Configure your advanced spoofing test scenarios

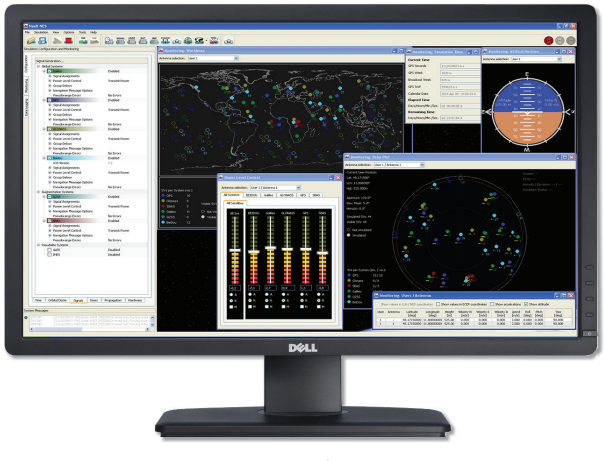

Contact IFEN for GNSS Test Equipment

In co-operation with

WORK MICROWAVE

IFEN

Americas
IFEN Inc.
+1 951 739 7331
M.Wilson@ifen.com

EMEA & APAC
IFEN GmbH
+49 8121 2238 20
sales@ifen.com

simulations were conducted using receivers mounted on ground and aerial vehicles.

Ground Receiver. The position of a receiver mounted on a ground vehicle was set to $r_r \equiv (10^6)\bullet[-2.431171, -4.696750, 3.553778]^T$ expressed in an Earth-Centered-Earth-Fixed (ECEF) coordinate frame. The elevation and azimuth angles of the GPS SV constellation above the receiver over a 24-hour period was computed using GPS SV ephemeris files from the Garner GPS Archive. The elevation mask was set to $el_{sv,min} \equiv 20°$. The azimuth and elevation angles of three SOPs, which were calculated from surveyed terrestrial cellular CDMA tower positions in the navigating receiver's vicinity, were set to $az_{sop} \equiv [42.4°, 113.4°, 230.3°]^T$ and $el_{sop} \equiv [3.53°, 1.98°, 0.95°]^T$, respectively. The resulting VDOP, HDOP, GDOP, and associated number of available GPS SVs for a 24-hour period starting from midnight, Sept. 1, 2015, are plotted in **FIGURE 2**.

The following can be concluded from these plots. First, the resulting VDOP using GPS + N SOPs for $N \geq 1$ is always less than the resulting VDOP using GPS alone. Second, using GPS + N SOPs for $N \geq 1$ prevents large spikes in VDOP when the number of GPS SVs drops. Third, using GPS + N SOPs for $N \geq 1$ also reduces both

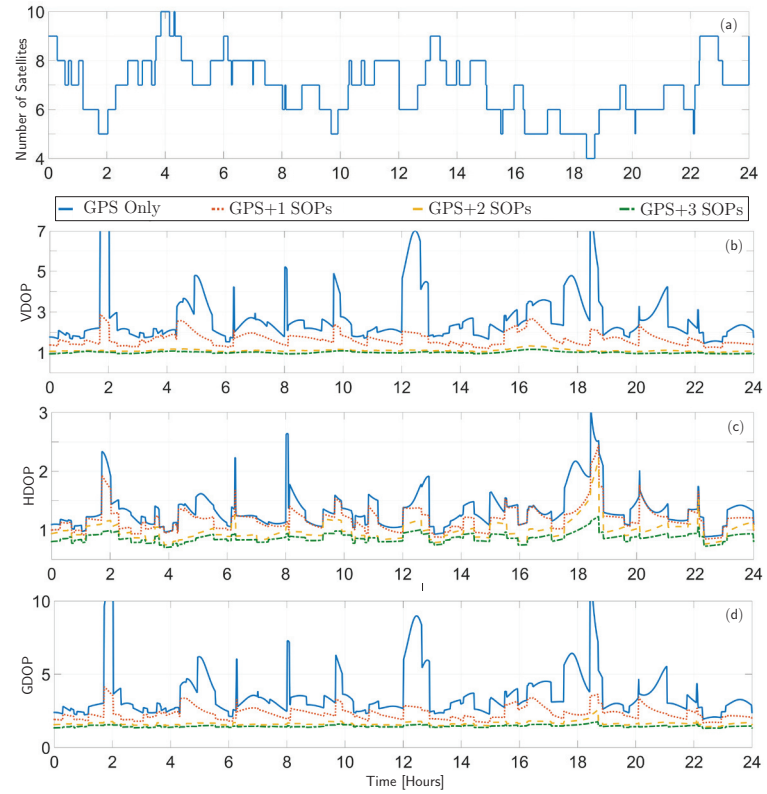

FIGURE 2 Fig. (a) represents the number of SVs with an elevation angle >20° as a function of time. Fig. (b)-(d) correspond to the resulting VDOP, HDOP, and GDOP, respectively, of the navigation solution using GPS only, GPS + 1 SOP, GPS + 2 SOPs, and GPS + 3 SOPs.

FIGURE 3 Simulation results for a UAV flying over downtown Los Angeles.
Top: Illustration of the true trajectory (red curve), navigation solution from using pseudoranges from six GPS SVs (yellow curve), and navigation solution from using pseudoranges from six GPS SVs and three cellular CDMA SOPs (blue curve).
Bottom: Illustration of uncertainty ellipsoid (yellow) of GPS only navigation solution and uncertainty ellipsoid (blue) of GPS + SOP navigation solution.

TABLE 2 DOP values for M + N SOPs.

(*M*) SVs, (*N*) SOPs: {*M*, *N*}	{4, 0}	{4, 1}	{4, 2}	{4, 3}	{5, 0}	{5, 1}	{5, 2}	{5, 3}
VDOP	3.773	1.561	1.261	1.080	3.330	1.495	1.241	1.013
HDOP	2.246	1.823	1.120	1.073	1.702	1.381	1.135	1.007
GDOP	5.393	2.696	1.933	1.654	4.564	2.294	1.880	1.566

HDOP and GDOP.

Unmanned Aerial Vehicle. The initial position of a receiver mounted on a UAV was set to $r_r \equiv (10^6)\bullet[-2.504728, -4.65991, 3.551203]^T$. The receiver's true trajectory evolved according to velocity random walk dynamics. Pseudorange observations on all available GPS SVs above an elevation mask set to $el_{sv,min} \equiv 20°$ and three terrestrial SOPs were generated using a MATLAB-based simulator. The simulator used SV trajectories which were computed using GPS SV ephemeris files from Sept. 1, 2015, 10:00 to 10:03 a.m.

The positions of the SOPs were set to $r_{sop(1)} \equiv (10^6)\bullet[-2.504953, -4.659550, 3.551292]^T$, $r_{sop(2)} \equiv (10^6)\bullet[-2.503655, -4.659645, 3.552050]^T$, and $r_{sop(3)} \equiv (10^6)\bullet[-2.504124, -4.660430, 3.550646]^T$, which are the locations of surveyed cellular towers in the UAV's vicinity. The UAV's true trajectory, navigation solution from using only GPS SV pseudoranges, and navigation solution from using GPS and SOP pseudoranges are illustrated in **FIGURE 3** (top). The corresponding 95th-percentile uncertainty ellipsoids for a sample set of navigation solutions are illustrated in Figure 3 (bottom).

The following can be noted from these plots. First, the accuracy of the vertical component of the GPS-only navigation solution is worse than that of the GPS + SOP navigation solution. Second, the uncertainty in the vertical component of the GPS-only navigation solution is larger than that of the GPS + SOP navigation solution, which is captured by the yellow and blue uncertainty ellipsoids, respectively. Third, the accuracy of the horizontal component of the navigation solution is also improved by incorporating cellular SOP pseudorange observations alongside

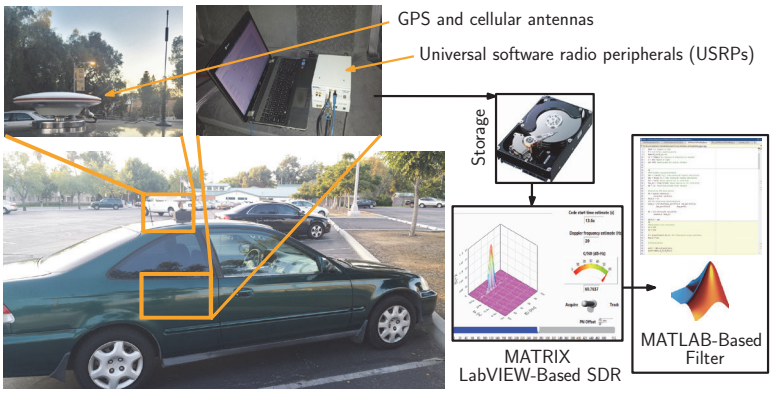

FIGURE 4 Experiment hardware setup.

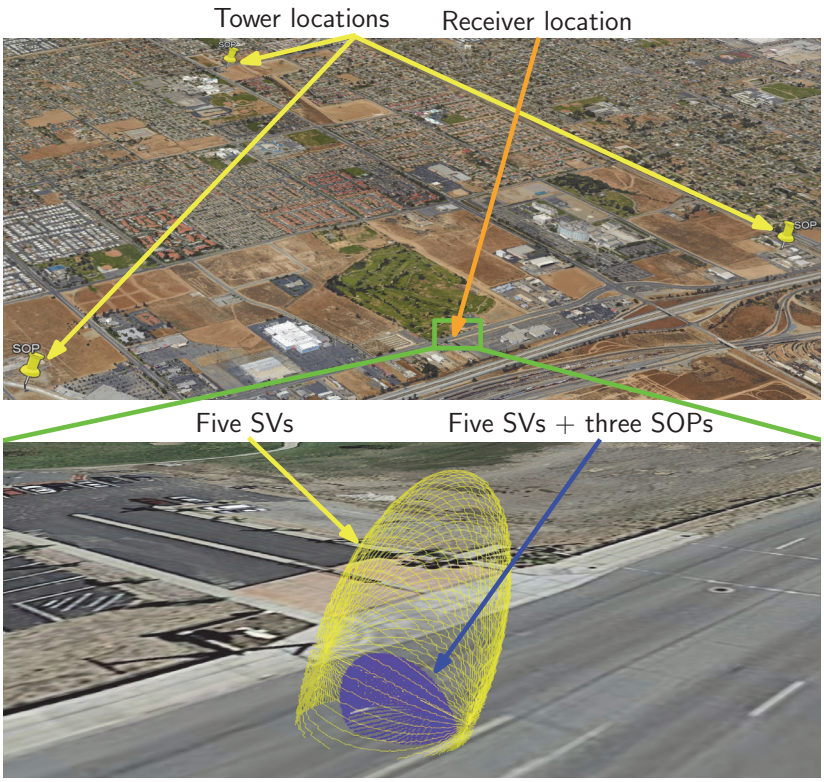

FIGURE 6 Top: Cellular CDMA SOP tower locations and receiver location. Bottom: Uncertainty ellipsoid (yellow) of navigation solution from using pseudoranges from five GPS SVs and uncertainty ellipsoid (blue) of navigation solution from using pseudoranges from five GPS SVs and three cellular CDMA SOPs.

GPS SV pseudorange observations.

EXPERIMENTAL RESULTS

A field experiment was conducted using software-defined receivers (SDRs) to demonstrate the reduction of VDOP obtained from including SOP pseudoranges alongside GPS pseudoranges for estimating the states of a receiver. To this end, two antennas were mounted on a vehicle to acquire and track multiple GPS signals and three cellular base transceiver stations (BTSs) whose signals were modulated through CDMA. The GPS and cellular signals were simultaneously downmixed and synchronously sampled via two universal software radio peripherals (USRPs). These front-ends fed their data to the Multichannel Adaptive TRansceiver Information eXtractor (MATRIX) SDR, developed at the Autonomous Systems Perception, Intelligence and Navigation (ASPIN) Laboratory at the University of California, Riverside. The LabVIEW-based MATRIX SDR produced pseudorange observables from five GPS L1 C/A signals in view and the three cellular BTSs.

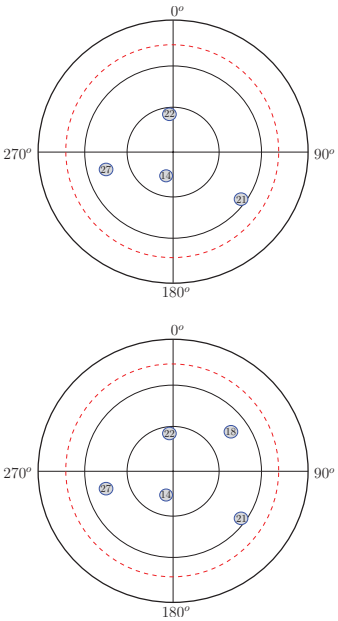

FIGURE 5 Top: Sky plot of GPS SVs: 14, 21, 22, and 27 used for the four SV scenarios. Bottom: Sky plot of GPS SVs: 14, 18, 21, 22, and 27 used for the five SV scenarios. The elevation mask, $el_{sv,min}$, was set to 20° (dashed circle).

FIGURE 4 depicts the experimental hardware setup.

The pseudoranges were drawn from a receiver located at $r_r \equiv (10^6) \bullet [-2.430701, -4.697498, 3.553099]^T$, expressed in an ECEF frame, which was surveyed using a carrier-phase differential GPS receiver.

The corresponding SOP state estimates were collaboratively estimated by receivers in the navigating receiver's vicinity. The pseudoranges and SOP estimates were fed to a least-squares estimator, producing $\hat{x}_r$ and associated P from which the VDOP, HDOP, and GDOP were calculated and tabulated in **TABLE 2** for M GPS SVs and N cellular CDMA SOPs. A sky plot of the GPS SVs used is shown in **FIGURE 5**. The tower locations, receiver location and a comparison of the resulting 95th-percentile estimation uncertainty ellipsoids of $\hat{x}_r$ for $\{M,N\}=\{5,0\}$ and $\{5,3\}$ are illustrated in **FIGURE 6**. The corresponding vertical error was 1.82 meters and 0.65 meteres respectively. Hence, adding three SOPs to the navigation solution that used five GPS SVs reduced the vertical error by 64.3 percent. Although this is a significant improvement over using GPS observables alone, improvements for aerial vehicles are expected to be even more significant, since they can exploit a full span of observable elevation angles as demonstrated in the simulation section.

CONCLUSION

This article studied the VDOP reduction of a GNSS-based navigation solution by exploiting terrestrial SOPs. It was demonstrated that the VDOP of a GNSS solution can be reduced by exploiting the inherently small elevation angles of terrestrial SOPs. Experimental results using ground vehicles equipped with SDRs demonstrated VDOP reduction of a GNSS navigation solution by exploiting a varying number of cellular CDMA SOPs. Incorporating terrestrial SOP observables alongside GNSS SV observables for VDOP reduction is particularly attractive for aerial systems, since a full span of observable elevation angles becomes available.

MANUFACTURERS

Two National Instruments universal software radio peripherals were used in the experiment. A Trimble 5700 receiver surveyed the experimental receiver location.

JOSHUA J. MORALES is pursuing a Ph.D. in electrical and computer engineering at the University of California, Riverside.

JOE J. KHALIFEH is a Ph.D. student at the University of California, Riverside.

ZAHER (ZAK) M. KASSAS is an assistant professor at the University of California, Riverside. He received a Ph.D. in electrical and computer engineering from the University of Texas at Austin. Previously, he was a research and development engineer with the LabVIEW Control Design and Dynamical Systems Simulation Group at National Instruments Corp.

This article is based on a technical paper presented at the **2016 ION ITM** conference in Monterey, California.